

## Pulse Transient Method as a Tool for the Study of Thermal Properties of Solar Cell Laminating Films

O. Zmeškal · P. Štefková · L. Hřebenová · R. Bařinka

Received: 5 March 2009 / Accepted: 17 November 2009 / Published online: 26 November 2009  
© Springer Science+Business Media, LLC 2009

**Abstract** The paper reports a study on the possible influence of surroundings on thermal properties of various types of laminating films used in the design of photovoltaic (PV) modules based on crystalline silicon. The main purpose of cell encapsulation is to provide protection of PV panels against environmental damage (especially humidity). However, the laminating film can influence also the electrical behavior of the whole panel because of differences in the working temperature. It is well known that with increasing solar cell temperature the PV conversion efficiency is decreasing. Therefore, it is important to study the thermophysical properties of laminating foils which are used for PV cells encapsulation. These materials must possess low specific heat and high thermal conductivity. Therefore, by using a laminating film with low absorption, high thermal conductivity, and high emissive ability of the rear (not illuminated) side, the PV module working temperature can be lowered and thus the generated power is increased and the investment recovery time shortened. The method of measurement is relative. The goal is not to determine the thermophysical parameters of laminating foils, but only to compare the influence of selected types of laminating foils on heat flow from the PV panel. A planar heat source placed between two PMMA blocks with defined thermal properties was adopted as the model of a real PV panel. A measurement on real PV panels was carried out by thermal imaging with a thermocamera. The correlation between both measurements was found.

---

O. Zmeškal (✉) · P. Štefková · L. Hřebenová  
Faculty of Chemistry, Institute of Physical and Applied Chemistry, Brno University of Technology,  
Purkyňova 118, 61200 Brno, Czech Republic  
e-mail: zmeskal@fch.vutbr.cz

R. Bařinka  
Solartec s.r.o., Televizní 2618, 756 61 Rožnov pod Radhoštěm, Czech Republic

**Keywords** Fractal analysis · Fractal structure · Specific heat · Thermal conductivity · Thermal diffusivity · Thermo vision · Transient pulse method

## 1 Introduction

This study deals with the use of a new data evaluation method, which was described in [1]. The method results from generalized relations that were designed for study of physical properties of fractal structures [2,3]. As is shown, these relations are in good agreement with the equations used for the description of time responses of the temperature for the pulse input of supplied heat [4–6]. Comparable outcomes of thermal parameters (specific heat, thermal diffusivity, and thermal conductivity) with a classical method were obtained.

The method was applied for comparison of thermal properties of various kinds of laminating films (two-colors: F02, F07, glow-matting: F03, F04, F06, and transparent: F05, F08, F09). Figure 1 shows their arrangement at the photovoltaic (PV) panel.

Figure 2 shows the results of preliminary measurements of thermal properties of a PV panel under halogen lamp illumination. There is a thermograph of the PV panel with PV cells covered by different laminating films in this figure. This thermograph, from 28 °C to 50 °C, shows the heat accumulated in the specimens (laminating films). It is evident that laminating films F05, F08, and F09 have much lower temperature than the others (it means these carry off the most heat from the PV cell). On the other hand, laminating films F04 and F06 embody the worst properties (it means these carry off the least heat from the PV cell).

The two-color laminating film F07 (blue–white) carries off heat better, if the white side is in contact with the PV cell. It is possible to expect that also the two-color

**Fig. 1** Arrangement of PV panel

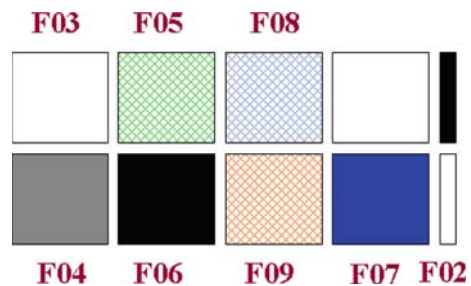
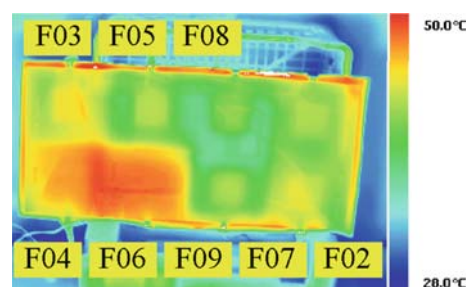


**Fig. 2** Thermograph of PV panel with PV cells covered by different laminating films



laminating films F02 (black–white) that are not placed under a PV cell will demonstrate similar properties.

The aim of this paper is to confirm these results by means of a detailed quantitative assessment of measurements using the pulsed transient method.

A planar heat source inserted between two PMMA blocks with defined thermal properties was used as a defined real heat source simulating a PV module. The goal was to identify the differences in thermal properties of the studied structures after the insertion of laminating foils. It is possible to evaluate the suitability of the studied laminating foils in a real PV panel design based on these experimental results. This arrangement of measurement was chosen due to the difficulties associated with measuring thermal properties of thin laminating foils and the impossibility of using the ideal model for heat transport through such films.

## 2 Theory

The fractal theory of the description of thermophysical properties is derived, in general, from integral transformations. It can describe the dependence of the change in physical quantities (e.g., in our case the temperature) on the energy (e.g., heat) transport process through a material. The trend of change can be expressed by the parameter  $D$  (so called fractal dimension). This parameter has different values for different integral transformations. The box counting fractal dimension is calculated, e.g., from a wavelet Haar transformation. It has local character and is used for image analysis.

The fractal dimension can describe the average change of properties of a physical quantity (e.g., temperature) in the whole material (it has a global character) when we used the Fourier transformation for the calculation. The results for the special cases (point, linear, and planar heat source—Dirac pulse) and a homogeneous infinite material were derived from a system of differential equations [4–6]. The fractal dimension expresses the character (dimension) of the heat source ( $D = 1, 2, 3$ ).

Different corrections (to pulse width and energy, to the thickness and finite surface area, to the heat source specific heat) and limited conditions for using theoretically derived equations are used for real cases (inhomogeneous heat source) and inhomogeneous (composites, structured) materials, see [7–10].

The fractal dimension gives information about the properties of a real heat source (immediately after heating) and about the heat drain from the material to the surroundings in this case. The fractal dimension will be in the interval  $D \in (1, 2)$  for a planar heat source and cylindrical sample.

The dependence of the fractal structures' temperature (characterized by the fractal dimension  $D$  in  $E$ -dimension space) on the distance from the heat source  $h_T$  and on the time  $t$  was determined in [1] using the theory of the space–time fractal field [2, 3];

$$T = \frac{Q}{c_p \rho (4\pi at)^{(E-D)/2}} \exp\left(-\frac{h^2}{4at}\right), \quad (1)$$

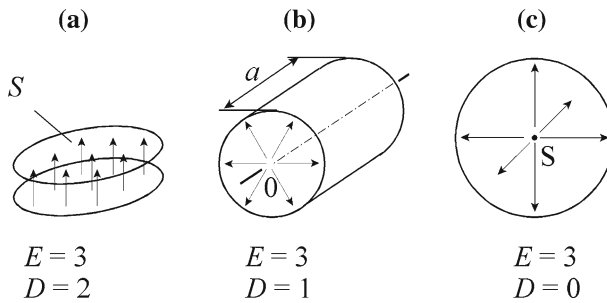


**Fig. 3** Heat flow geometry for (a) plane-parallel, (b) cylindrical, and (c) spherical coordinates Euclidean space

In this equation,  $Q$  is the heat supply from the heat source,  $c_p$  is the specific heat at constant pressure,  $\rho$  is the mass density, and  $a$  is the thermal diffusivity. The thermal conductivity,  $\lambda = c_p \rho a$ , can be calculated from these parameters. Equation 1 is applicable for fractal dimensions  $D = 0, 1, 2$  and topological dimension  $E = 3$  [4–6], see Figs. 3 and 4.

The maximum position can be determined by differentiation of Eq. 1 with respect to time,

$$\frac{\partial \log T}{\partial \log t} = \left( \frac{D - E}{2} + \frac{h^2}{4at} \right) = 0 \quad (2)$$

From this equation, the thermal diffusivity at the time of the maximum can be determined;

$$a = \frac{h^2}{2t_m f_a} = \frac{h^2}{2(E - D)t_m} \quad (3)$$

where  $f_a$  is a coefficient that characterizes the deformation of the thermal field [6]. This coefficient is equal to one for the ideal planar source ( $E = 3, D = 2$ ). The maximum temperature of the response for a Dirac thermal pulse is obtained by introduction of the thermal diffusivity, Eq. 3 and 1;

$$T_m = \frac{Q}{c_p \rho} \exp\left(\frac{D - E}{2}\right) \left(\frac{E - D}{2\pi h^2}\right)^{(E-D)/2} \quad (4)$$

From the ratio of Eqs. 4 and 1 and with the use of the Eq. 3,

$$\frac{T_m}{T} = \left[ \frac{t}{t_m} \exp\left(\frac{t_m}{t} - 1\right) \right]^{\frac{E-D}{2}}, \quad (5)$$

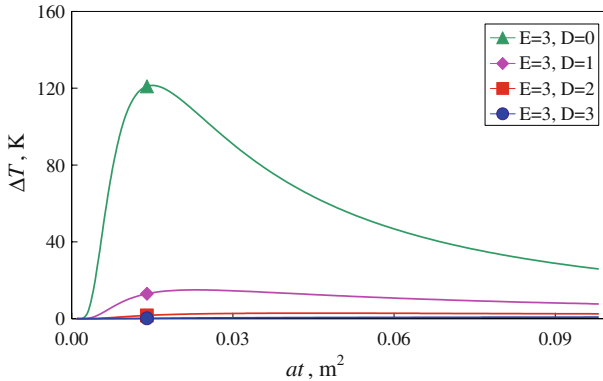


**Fig. 4** Time dependence of the temperature response for the Dirac thermal pulse calculated by Eq. 1 for the heat flow geometry from Fig. 3

it is possible to define the coefficient  $f_a$  (fractal dimension  $D$ , respectively) for every point of the experimental relationship,

$$f_a = E - D = \frac{2 \ln(T_m/T)}{\ln(t/t_m) + (t_m/t - 1)}. \tag{6}$$

The value of the coefficient  $f_a$  could also be affected by the geometry of the sample [6] or by the finite pulse width [7].

In the case of the studied fractal structure, one can derive formulas using Eq. 4 for the specific heat,

$$c_p = \frac{Q}{\rho T_m h T} \frac{f_c}{\sqrt{2\pi \exp(1)}} = \frac{Q}{\rho T_m h E^{-D}} \left( \frac{E - D}{2\pi \exp(1)} \right)^{(E-D)/2} \tag{7}$$

and the thermal conductivity

$$\lambda = c_p \rho a = \frac{Q}{2(E - D) T_m t_m h E^{-D-2}} \left( \frac{E - D}{2\pi \exp(1)} \right)^{(E-D)/2} \tag{8}$$

where  $f_a$  and  $f_c$  are the coefficients that characterize the deformation of the thermal field [6].

Equation 5 represents time–temperature dependences (according to Eq. 1) calculated for spherical ( $D = 0$ ), cylindrical ( $D = 1$ ), planar ( $D = 2$ ), and cubic ( $D = 3$ ) geometries of the heat source (see Fig. 3). It is evident from Eqs. 5 and 2 that for  $D = E$  the function becomes a maximum as  $t \rightarrow \infty$ .

All dependences for the long time intervals converge to the asymptote, which is longitudinal with the time scale. The intersection of this asymptote with the vertical scale determines the coefficient  $f_a = (E - D)$  and thus the fractal dimension  $D$  that characterizes the specimen setup (heat source, specimen, distribution of the temperature field, heat losses). When the value of  $f_a$  is known, it is feasible to determine the

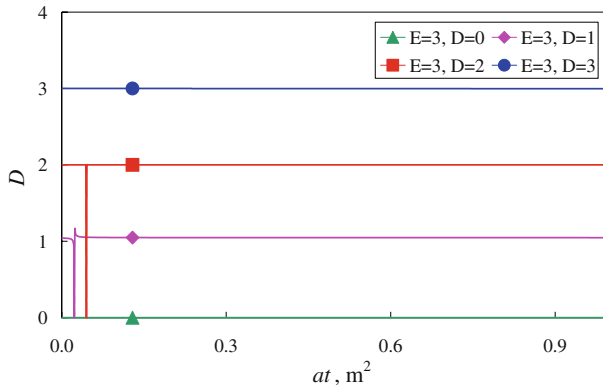


**Fig. 5** Time dependence of the reconstructed fractal dimension  $D$  for the Dirac thermal pulse and the heat flow geometry from Fig. 3 calculated using Eq. 6

thermophysical parameters of the studied thermal system with the aid of Eqs. 3, 4, 5, 6, 7, and 8.

The source type reconstruction (its fractal dimension  $D$  and coefficient  $f_a$ ) can be determined using Eq. 6. The calculated time dependences of these fractal dimensions for all four cases are shown in Fig. 5. One can see that the results are in agreement with the input parameters. Discrepancies due to numerical errors in the calculation using Eq. 6 are only for  $t \approx t_m$ .

### 3 Experimental

The Thermophysical Transient Tester 1.02 was used for measuring the responses to the pulse heat. It was developed at the Institute of Physics, Slovak Academy of Science [11]. The setup of the experiment is described in [6].

Thermal responses were used for the data evaluation. Three possible configurations of the experiment arrangement are shown in Fig. 6. Figure 6a shows the arrangement when the diameter of a specimen is equal to the diameter of the heat source. On the other hand, Fig. 6c depicts the experimental setup with the diameter of the heat source being significantly smaller than the specimen diameter. Figure 6b shows the real situation, when the heat is delivered irregularly (either from the source of finite size or from a source with a specific composition of heat sources).

The measured sample of PMMA was disc-shaped with a diameter  $R = 0.03$  m and thickness  $h = 6.0$  mm. Its density was  $\rho = 1184$  kg  $\cdot$  m<sup>-3</sup>, the thermal diffusivity  $a = 1.12 \times 10^{-7}$  m<sup>2</sup>  $\cdot$  s<sup>-1</sup>, the specific heat  $c_p = 1450$  J  $\cdot$  kg<sup>-1</sup>  $\cdot$  K<sup>-1</sup>, and the thermal conductivity of the sample was  $\lambda = 0.193$  W  $\cdot$  m<sup>-1</sup>  $\cdot$  K<sup>-1</sup>.

The comparison of laminating films properties was carried out by means of inserting them between the heat source and the measured reference material (PMMA), see Fig. 7. In Fig. 7a, the structure of a real PV cell from Fig. 2 is shown. The PV cell was replaced by the heat source in Fig. 7b, c. Measurements of the thermal parameters of the system formed by PMMA and the laminating films were carried out for this arrangement.

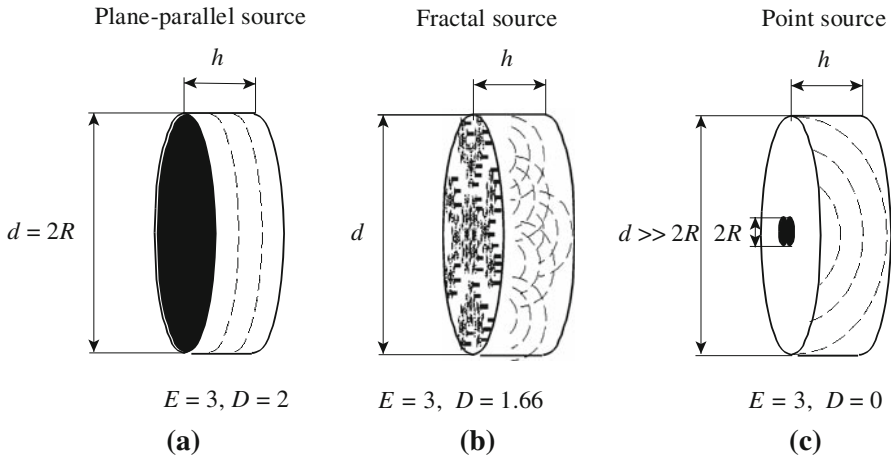


**Fig. 6** Current flow geometry: (a) plane-parallel, (b) fractal, and (c) point (for different ratios of length contact, respectively) source

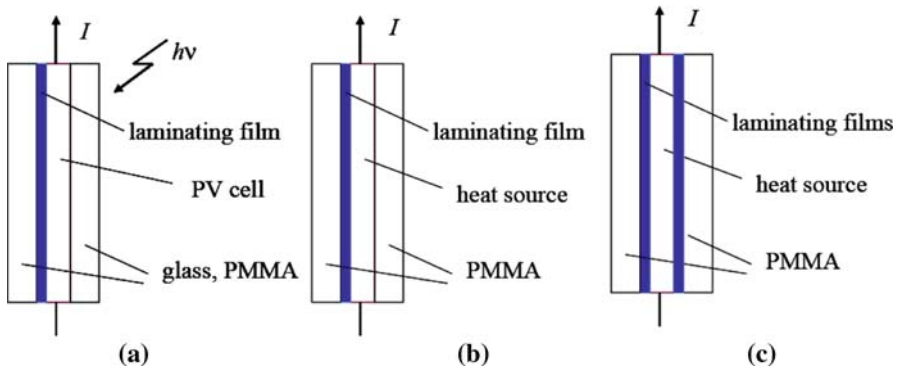


**Fig. 7** Arrangement of thermal system for measuring properties of laminating films: (a) real PV cell as heat source, and (b) and (c) model with laminating films from one or both sides of the heat source

### 4 Results

Typical time responses of the temperature for the pulse of input power are represented in Fig. 8. The width of the heat pulse was  $\Delta t = 28$  s, and the pulse energy covered the range from  $15 \text{ kJ} \cdot \text{m}^{-2}$  to  $40 \text{ kJ} \cdot \text{m}^{-2}$ . It is evident that the maximum of this dependence increases with the heat power.

The basic parameters calculated from the dependences in Fig. 8 are presented in Table 1. The values of the heat energy for a unit area of the source to the sample are in the first column. Results for pulses of  $\Delta t = 4$  s width and different powers are in the first four rows; in the last row, a  $\Delta t = 100$  ms pulse width is used. In the second and third columns, the time and temperature of maximum dependences in Fig. 8 are listed. Time constants calculated from exponential dependences of the fractal dimension on the heat source energy are given in the fourth column. The last three columns give

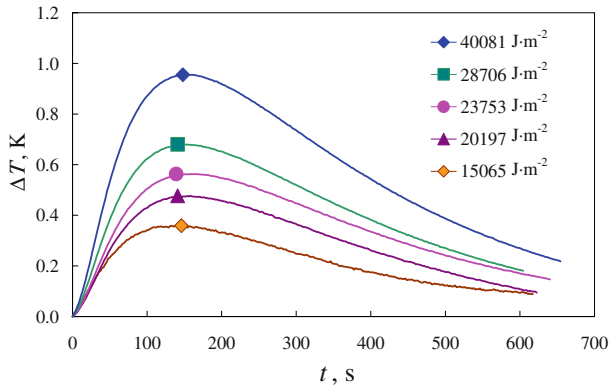


**Fig. 8** Thermal responses of the sample measured by the pulse transient method. Measurements were carried out for different heat powers and a pulse width  $\Delta t = 28$  s

**Table 1** Measured and calculated parameters from measured characteristics

$Q/S$ ( $\text{J} \cdot \text{m}^{-2}$ )	$t_m$ (s)	$\Delta T_m$ (K)	$a \times 10^7$ ( $\text{m}^2 \cdot \text{s}^{-1}$ )	$c_p$ ( $\text{J} \cdot \text{kg}^{-1} \cdot \text{K}^{-1}$ )	$\lambda$ ( $\text{W} \cdot \text{m}^{-1} \cdot \text{K}^{-1}$ )
15065	146	0,359	0.115	1405.8	0.191
20197	141	0.477	0.120	1419.1	0.202
23753	139	0.563	0.124	1414.1	0.207
28706	141	0.680	0.123	1415.2	0.207
40081	148	0.955	0.115	1405.6	0.192
			$0.119 \pm 0.004$	$1412.0 \pm 6.0$	$0.200 \pm 0.008$

basic values which characterize the thermal properties of materials: thermal diffusivity  $a$ , specific heat  $c_p$ , and thermal conductivity  $\lambda$ .

It is evident from these results that the determined thermal parameters of PMMA are close to the parameters from the literature; see Sect. 3 and Refs. [8–10].

The results obtained from the measurement of the system after the insertion of laminating films will be discussed in the next section, see Fig. 7. Figure 9 clearly illustrates that the maximum temperature of the measured pulse decreases, and it shifts to lower values.

The higher specific heat of the system with a laminating film results from this fact. We can also determine its higher thermal conductivity after a more detailed analysis.

It is evident from the dependence of coefficient  $D$ , Eq. 6, that the contact between the heat source and the measured material was not ideal in any case; it is possible to characterize it by a value  $D \approx 1.5$ . This divergence is probably caused by thermal losses into the environment. The results (see Fig. 10) of the thermal conductivity and specific heat of the measured systems PMMA–laminating films (F02–F09) are compared in the last two figures. It is evident from Fig. 11 that for a majority of the measured materials, the thermal conductivity of the system is higher than that of the PMMA (red column-F01). From this point of view, these are suitable specimens for application as laminating films. However, the situation is slightly more difficult



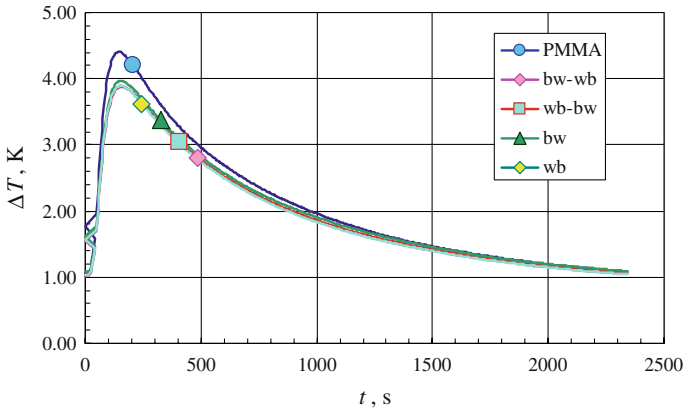


**Fig. 9** Thermal responses of the sample measured by the pulse transient method without using (PMMA) and with using blue-white laminating film from one (bw, wb) and both sides of heat source (wb–bw, bw–wb)

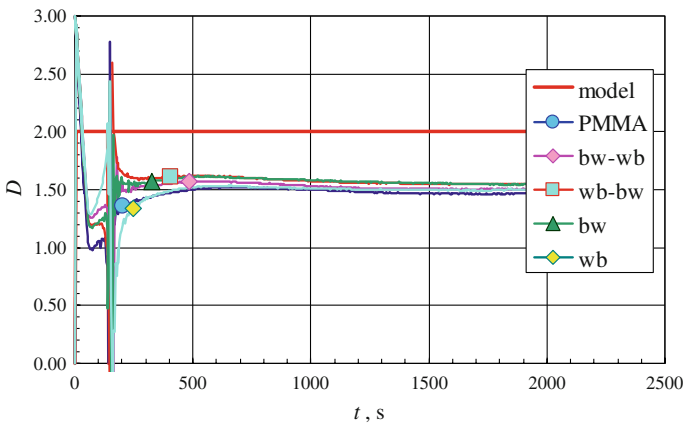


**Fig. 10** Dependence of fractal parameter  $D$  calculated from transient response of all points of measurements. Measurements were carried out for all characteristics in Fig. 9

when the specific heat is considered (Fig. 12). Suitable materials should have the specific heat of the PMMA–laminating film much smaller than the specific heat of only PMMA.

Only transparent materials can fulfill this condition (laminating films F05, F08, F09). On the other hand, the specific heat of black–white film (F02) and black film (F06) is very high, and they are not suitable for application as heat removing elements in PV panels. The results of measurements by means of the pulse transient method confirmed estimates carried out on the basis of measurements of the temperature distribution by means of a thermocamera.

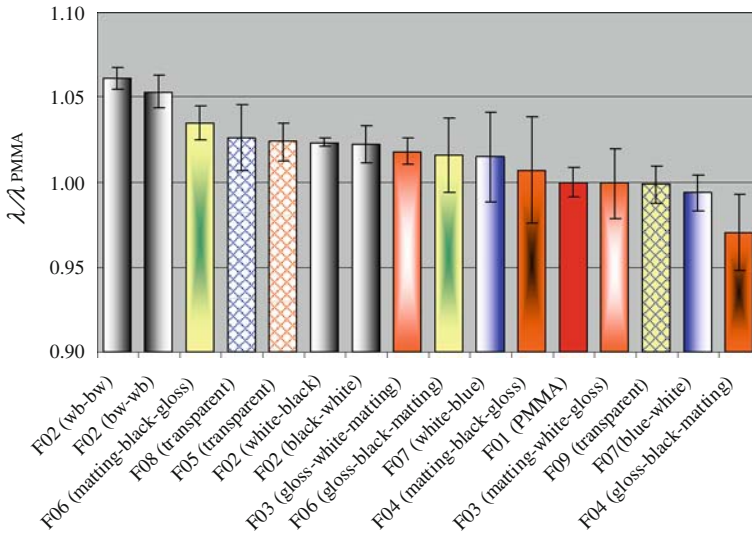


**Fig. 11** Summary of results of thermal-conductivity relative values of system of PMMA-laminating films to the thermal conductivity of PMMA (*red column*)

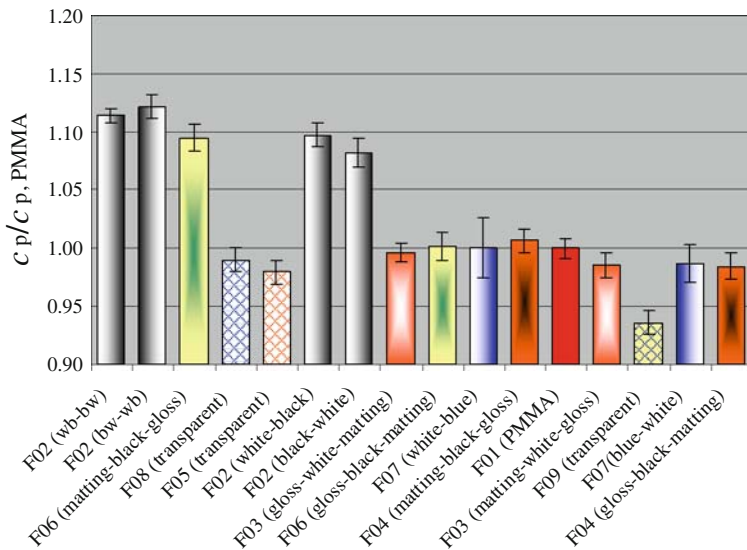


**Fig. 12** Summary of results of specific-heat relative values of system of PMMA-laminating films to the specific heat of PMMA (*red column*)

### 5 Conclusion

In this study, results evaluated from thermal responses to a heat pulse are discussed. To interpret the findings, a simplified thermal conductivity model is used [1]. The model is based on work published in [4]. Results showed the image of heat distribution in a

specimen for various time intervals after the exposure to heat from the source. These evaluations could be used for more accurate determination of the thermal parameters of the studied materials.

Properties of various types of laminating films used for the encapsulation of cells of PV panels were compared in the second part. The results gained by measurements of the temperature distribution using a thermocamera were confirmed and quantitatively compared.

**Acknowledgments** This work was supported by project KAN401770651 from The Academy of Sciences of the Czech Republic and by project and by grants FT-TA3/048 and FR-TI1/144 from the Ministry of Industry and Trade of the Czech Republic.

## References

1. P. Štefková, O. Zmeškal, R. Capoušek, in *Complexus Mundi* (World Scientific, London, 2006), p. 217. ISBN 981-256-666-X
2. O. Zmeškal, M. Nežádal, M. Buchnřek, *Chaos Solitons Fractals* **17**, 113 (2003)
3. O. Zmeškal, M. Nežádal, M. Buchnřek, *Chaos Solitons Fractals* **19**, 1013 (2004)
4. H.S. Carslaw, J.C. Jaeger, *Conduction of Heat in Solids* (Clarendon Press, London, 1959), p. 496
5. J. Krempaský, *Measurement of Thermophysical Quantities* (VEDA, Bratislava, 1969), p. 287
6. L. Kubičár, *Pulse Method of Measuring Basic Thermophysical Parameters* (VEDA, Bratislava and Elsevier, Amsterdam, 1990), p. 344
7. V. Boháč, L. Kubičár, V. Vretenár, in *Proceedings of TEMPMEKO 2004, 9th International Symposium on Temperature and Thermal Measurements in Industry and Science*, ed. by D. Zvizdić, L.G. Bermanec, T. Veliki, T. Stašić (FSB/LPM, Zagreb, Croatia, 2004), pp. 1299–1306
8. V. Boháč, L. Kubičár, V. Vretenár, *Meas. Sci. Rev.* **5**, 98 (2005)
9. V. Štofanič, M. Markovič, V. Boháč, P. Dieška, L. Kubičár, *Meas. Sci. Rev.* **7**, 15 (2007)
10. V. Boháč, P. Dieška, L. Kubičár, *Meas. Sci. Rev.* **7**, 24 (2007)
11. *Thermophysical Transient Tester—Model RT 1.02*, Institute of Physics, Slovak Academy of Sciences, Bratislava, Slovak Republic